LA-UR- 11-04099

Approved for public release; distribution is unlimited.

Title: Wind Turbines Research at Los Alamos National Laboratory – Integrating Experimental Aerodynamics, Sensing, Structural Mechanics and Numerical Simulations

Author(s): B. J. Balakumar, C. Ammerman, S. Pol, R. Linn, E. Koo, G. Ellis, G. Park, K. Farinholt, R. C. Alarcon

Intended for: 41st AIAA Fluid Dynamics Meeting
Honolulu, Hawaii
27-30 June 2011

Los Alamos
NATIONAL LABORATORY
EST.1943

Wind Turbines Research at Los Alamos National Laboratory – Integrating Experimental Aerodynamics, Sensing, Structural Mechanics and Numerical Simulations

B. J. Balakumar[1], C. Ammerman[3], S. Pol[1], R. Linn[2], E. Koo[2], G. Ellis[3], G. Park[4], K. Farinholt[3], R. C. Alarcon[5]
Los Alamos National Laboratory, Los Alamos, NM 87545

In support of the Department of Energy's goal of achieving 20% wind energy by 2030, Los Alamos National Laboratory's Intelligent Wind Turbine (IWT) project has developed and applied novel diagnostics, supercomputing simulation tools, custom-built sensing platforms and detailed structural models to study wind turbine reliability. These leaps in the current state-of-the-art include (a) Large Field of View and Rotating Particle Image Velocimetry diagnostics to resolve flow fields around wind turbines, (b) supercomputing simulations that incorporate complex terrains and resolve scales ranging from 2m to several Kms, (c) detailed blade models for aero-elastic simulations, and (d) structural health monitoring hardware and algorithms. Fusing information from different, independent techniques, the IWT project aims to develop an integrated framework for investigating turbine-turbine interactions and turbine reliability. Here, we report our recent progress in these areas, and discuss how these tools will be utilized effectively to understand aero-structural dynamics at LANL's Wind Turbine Field Station.

Nomenclature

HPC	=	High Performance Computing
CFD	=	Computational Fluid Dynamics
LLJ	=	Low Level Jet
LANL	=	Los Alamos National Laboratory
SNL	=	Sandia National Laboratories
NREL	=	National Renewable Energy Laboratory
NuMAD	=	Numerical Manufacturing And Design
GUI	=	Graphical User Interface
ACP	=	ANSYS Composite PrepPost
IWT	=	Intelligent Wind Turbine
V&V	=	Verification and Validation

I. Introduction

LOS Alamos National Laboratory's Intelligent Wind Turbine (IWT) project is a multi-disciplinary engineering research and development effort involving researchers in the areas of aerodynamics, sensing, structural mechanics and high performance computing. The aim of this project is to support the Department of Energy's goal of achieving 20% wind energy by 2030[1]. Applying novel new diagnostics, sensing technologies, and simulation platforms developed within Los Alamos during the last several years, this project has made significant inroads into the development of a unified framework for understanding turbine-turbine performance and plant-scale reliability.

[1] Physics Division, Los Alamos National Laboratory, SM30 Bikini Atoll Rd, Los Alamos, NM 87545
[2] Earth & Environmental Sciences Division, Los Alamos National Laboratory, SM30 Bikini Atoll Rd, Los Alamos, NM 87545
[3] Applied Engineering & Technology Division, Los Alamos National Laboratory, SM30 Bikini Atoll Rd, Los Alamos, NM 87545
[4] Engineering Institute, Los Alamos National Laboratory, SM30 Bikini Atoll Rd, Los Alamos, NM 87545
[5] Mechanical & Aerospace Engineering, New Mexico State University, Jett Hall, Las Cruces, NM 88003

This paper is a summary of some of our recent progress in integrating experimental aerodynamics, sensing, structural mechanics and numerical simulations.

The biggest obstacle to a viable, unsubsidized US wind industry is cost, currently at $35-60/MWh (and decreasing). Operation and maintenance (O&M) costs, however, climb steadily as wind plants age, starting out at about $5/MWh in the first year increasing to $15-20/MWh by year 20[2]. DOE's goal is to reduce these O&M costs by 40%[1]. The components most responsible for wind turbine unavailability (frequency of occurrence and length of downtime) are the gearbox (60%), generator (14%), and rotor blades (7%)[3]. One prominent factor that directly affects turbine reliability is the turbulence in the atmosphere. The inflow turbulence (including intermittent gusts) affects the instantaneous angle of attack between the incoming wind and the blade chords resulting in a local change in lift and drag forces. Depending on the spatial variation of the turbulence (two-point correlation), the load fluctuations across the blade might get averaged out or might get amplified. Recent progress in the study of coherent structures and very large scale motions in the atmosphere and other turbulent flows suggest that these load fluctuations are not well understood. Design criteria used currently for turbine designs are largely based on the European wind industry and do not reflect the more severe dynamic shear environments that occur in the US wind corridor[4].

The resolution of this strongly coupled aero-structural problem requires new developments in the measurement and modeling of both wind turbine aerodynamics and blade structural loadings. At LANL's IWT project, we are developing novel diagnostics based on Particle-Image Velocimetry (PIV) techniques that are capable of accurately measuring local inflow into the turbine, blade flows and near wake flows non-intrusively and in unprecedented detail. These measurements are used to validate high-fidelity LANL codes (WindBlade) that resolve blade scales from 2m to planetary scales of up to several Kms. The WindBlade code is designed with the goal of incorporating detailed aero-elastic structural responses into the simulation framework. To utilize this capability, we have also developed highly detailed blade structural models. In order to verify the aero-structural models, inexpensive, light-weight and embeddable active sensing platforms have been developed. In combination, these tools promise to provide a unified understanding of load fluctuations in wind turbines.

In this manuscript, we will discuss the challenges associated with the development of LF-PIV and R-PIV diagnostics and the solutions we have adopted to overcome these. This discussion is followed by details about LANL's simulation framework and some recent results of simulations of wind turbines located on complex terrains near Las Vegas, NM. Then, we will discuss the elastic blade model, and structural sensing solutions that will be used to validate our aero-elastic simulations. Some of the prominent results are discussed, although the nature of this discussion and the manuscript length precludes the possibility of detailed discussions. The readers are referred to other publications from the same team for more details about the results in each of the research areas.

II. Experimental Aerodynamics: Multi-Scale Experiments and Novel Diagnostics Development

The wind turbine research community has long felt a need for high-fidelity experimental measurements to validate numerical simulations and develop new models. Advanced diagnostics for measuring flows around wind turbines are thus far limited to three-axis sonic anemometers, Lidar systems (including hub-mounted rotating Lidars[5]), Sodars and satellite remote sensing[6]. Sonic anemometers have high accuracy but yield data only at a single point in the flow. Often, Taylor's hypothesis is used to extrapolate this data into a spatial dimension along a single line. Lidars and Sodars have a much larger range but are constrained by temporal and spatial resolution limitations. Further, there is general consensus that more understanding of the operations and errors associated with Lidars and Sodars are necessary[7]. There is also a strong need for experiments that compare the results between the various diagnostics, although some recent papers have addressed this research topic[8,9,10]. Yet another limitation is the unsuitability of current diagnostics for near blade measurements. For example, local inflow conditions cannot be measured non-intrusively with sonic anemometers. Although 5-hole pitot tubes have been used in the past, their performance and accuracy do not match those of hot-wires or Particle-Image Velocimetry (PIV) diagnostics, especially in the measurement of turbulence statistics[11]. Recently, hot-film measurements have been combined with sonic anemometers to measure local dissipation in planetary boundary layers, although such measurements are once again limited to single points in the flow field[12]. Further separated flow fields around rotating wind turbines operating under yawed conditions have only been investigated using smoke flow, surface pressure sensors or string markers [x]. This precludes the possibility of measuring the large scale structures shed by blades under conditions of dynamic stall and does not provide a detailed picture of stall or wake-turbine interactions.

At LANL, we have focused our efforts on developing novel diagnostics that can be used to understand conditions of dynamic stall and flows around wind turbine blades under yaw. As a part of this effort, we have developed a Large Field of View Particle Image Velocimetry (LF-PIV) diagnostic that is capable of accurately measuring flow fields over large regions. PIV diagnostics are typically limited to small fields of view in gases (of the order of a few centimeters in each dimension) due to particle size limitations. At LANL, we have demonstrated a

PIV field of view of more than 4.3m x 1.0 m using light, hollow polymer particles. Such a large field of view allows the possibility of capturing coherent structures around wind turbines under wind tunnel or field conditions. In addition, spatial correlations and the small scale structure of the turbulence can also be measured in great detail using this diagnostic. We have also developed a unique Rotating Particle Image Velocimetry (R-PIV) diagnostic that can be mounted on the hub of the wind turbine to measure velocity fields around blades operating under dynamic stall at all blade phase angles (in both rotation and pitch). These two unique techniques will be fielded at LANL's wind turbine field station that is currently under construction (and is expected to be completed towards the end of July) to provide unique, state of the art data on turbine-turbine interactions and turbine operations under yawed inflow conditions. The following sections provide more details about the capability, performance and challenges involved in the development of these diagnostics.

A. Large Field of View Particle Image Velocimetry (LF-PIV)

Particle-Image Velocimetry has provided important insights into the physics of various classes of fluid flows[13] due to its robust nature and ability to capture 2-D or 3-D velocity fields. And yet, in the field of wind turbines research, the use of PIV has generally been limited to wind tunnel scaled model experiments thus far[14]. This is primarily due to limitations in the field of view of PIV systems when they are used in gases. In gas flows, to ensure that particles track the fluid flows accurately, the particles are required to be small (of the order of 1 μm). For small particles, the Mie scattering intensity drops approximately as the square of the particle diameter, and hence, smaller particles are harder to record on an imaging device. Thus, to keep the recorded particle signal to noise ratio high, PIV diagnostics often operate under small fields of view in gases.

One approach to solving this bottleneck is the use of more powerful laser beams. Such laser systems, although available commercially, are prohibitively expensive. They also become bulky and are unsuitable for field deployment due to safety concerns. Yet another approach is the use of forward scattered light instead of side scatter[15]. This approach would result in distorted images and require the cameras to operate under small apertures (due to depth of field limitations). At LANL, we have taken the approach of using large particles to increase the scattered intensity, and using side scatter to record the images without perspective distortions (typical high end camera lenses have negligible pincushion or barrel distortions at the low magnifications we operate under). This results in substantially increased fields of view for PIV systems and brings flow fields around 2-20+m wind turbines accessible for PIV diagnostics.

Prior to fielding the diagnostic in the field, an investigation of the errors associated with the use of large particles in LF-PIV was carried out under laboratory conditions. The LF-PIV diagnostic was tested on a confined vortex flow created inside a 1.4m x 1.4m tank with suitably located fans. One advantage of using side-scatter over forward-scatter is the use of such laboratory-scale tanks for the analysis of diagnostic errors. It is easy to see (using Fresnel equations) that the side glass windows under shallow forward scatter angles would result in substantial loss of signals. Under such conditions, the forward scattered angle and the laser light sheet polarization must be tuned to take advantage of Brewster's law[16]. In our current case, such effects are not critical and the design becomes simple.

Sample mean flow field measurements performed in the glass tank using 2MP and 11MP cameras are shown in Figure 1. A model of a 4.5m blade (similar in size to a Whisper 500 blade but designed using blade element momentum theory) is also shown for comparison of measurement dimensions. It must be noted that our field of view is much larger than the size of the apparatus. Therefore, we moved our apparatus across the camera's field of view without changing the laser light sheet to determine the maximum measurable field of view. Based on our light sheet height, we could measure fields of up to 4.3m x 1.0m although a strong signal intensity recorded in the current set up implies that the light sheet could be made taller to measure even larger regions. For hollow plastic particles of 80 μm diameter, the maximum percentage slip was about 1.15% for an acceleration of 100g, g is the acceleration due to gravity, implying that the large particles are capable of tracking the flow fields with only small errors. Further details about the results and design guidance for implementing LF-PIV diagnostics are provided elsewhere[17].

B. Rotating Particle Image Velocimetry (R-PIV)

Flows around wind turbine blades under dynamic stall and separation are not well understood. Significant challenges in modeling these flows remain (due to the sensitivity of separation to inflow turbulence for e.g.) and measurements are limited to flow visualization and surface pressure measurements. We have developed a powerful new rotating PIV diagnostic that is capable of remotely obtaining PIV data around rotating airfoils under laboratory and field conditions. One of the unique aspects of this diagnostic is the capability to measure flow fields around turbine blades in-situ at all angles of rotation. This is achieved by mounting the camera and associated electronics on the turbine hub and routing the laser light, power and signals through the blades using rotating electro optical joints.

Since the coherent laser radiation used for PIV measurements often burn the fiber couplings, several trial and errors were required before the identification of suitable optics that can be used in the R-PIV apparatus. Controlling the camera focus while the camera is rotating several feet above the ground was another challenge. This was overcome using a novel gearing arrangement that can be controlled from the ground. Custom-built, turbine mounted solid state computers with no moving parts were used for remote data acquisition. The system will be tested shortly at LANL's wind turbine field station.

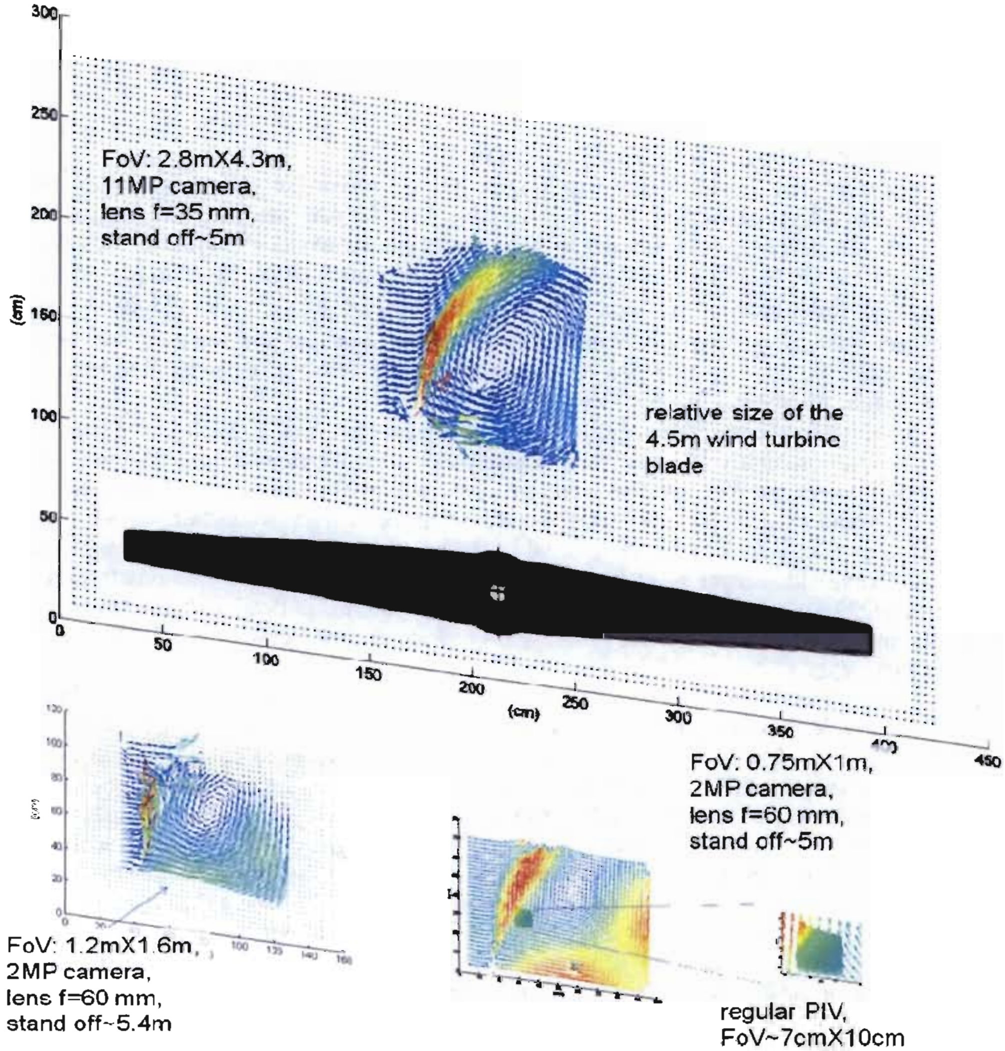

Figure 1: A mean LF-PIV velocity vector field at scale compared to a 4.5m diameter wind turbine design (similar to the Whisper 500 turbines that will be used at LANL's wind turbine field station). Large stand off distances and large fields of view are obtained using the LF-PIV apparatus. The flow tracking accuracy is within 2% for moderately strong vortices (~100g centrifugal accelerations). A comparison of the field of views between LF-PIV and regular PIV is also shown (bottom).

C. LANL Wind Turbine Field Station

The aerodynamic and structural data acquisition is expected to commence shortly at LANL's wind turbine field station. The diagnostics have been successfully tested under laboratory conditions and will be ported to test their operations under field conditions. A schematic of LANL's field station is shown in Figure 3.

The field station towers are designed to DoE specifications and the station is currently capable of mounting three 4.5m turbines with full and partial overlaps between turbine rotation planes to study (i) single turbine performance under complex inflow conditions and (ii) turbine-turbine interactions. The towers are overdesigned and can potentially carry larger turbines of up to 10m in diameter. Sensors towers are located 3D upstream, and 3D and 7D downstream of the primary turbine. All towers are designed to be tilt-down or telescopic for ease of diagnostics installation and maintenance. Diagnostics include standard CSAT3 sonic anemometers, RM Young sonic anemometers, LF-PIV, R-PIV systems and extensive structural health monitoring systems. This field station is capable of measuring fatigue damage propagation and correlating it to aerodynamic effects (e.g. gusts). A nearby 60m met tower provides additional measurements of the flow conditions at higher altitudes above the field station. Collaborations from Universities to field other diagnostics (e.g. Sodar) are also underway. The field station is expected to be completed in late July.

Figure 2: Photograph of LANL's Rotating PIV apparatus (Patent in progress). The diagnostic is designed to capture blade boundary layers under dynamic stall at any phase angle of rotation. This apparatus is also capable of non-intrusively measuring local blade inflow conditions.

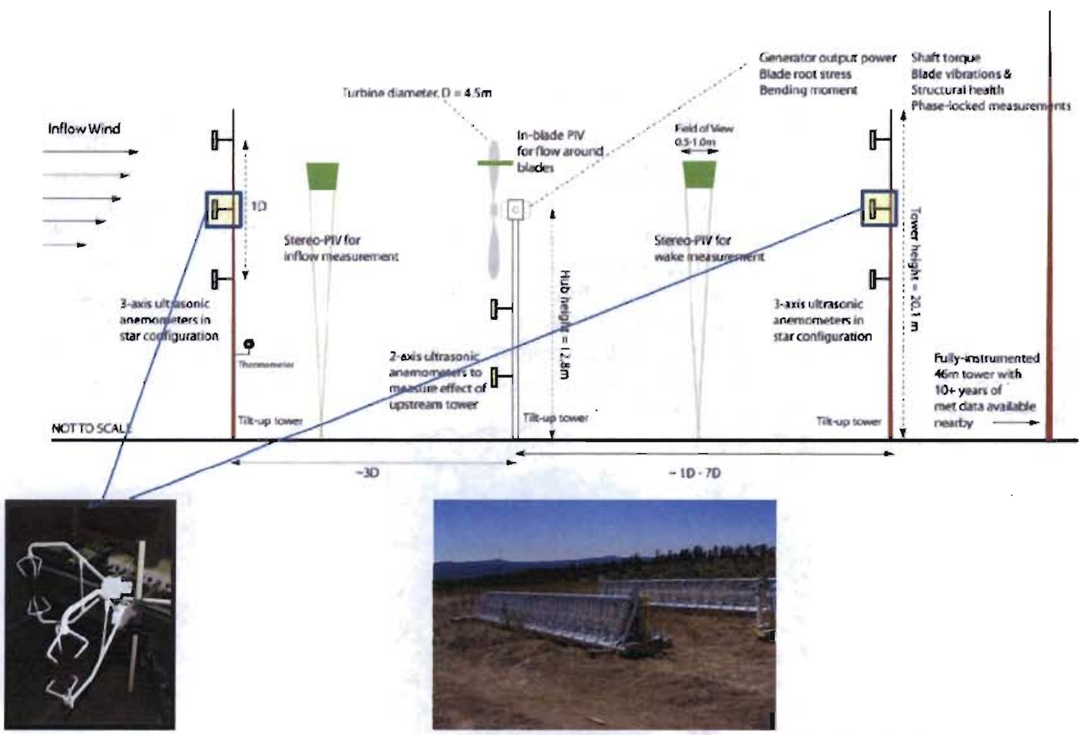

Figure 3: (above) Schematic of the LANL field station to investigate turbine-turbine interactions under complex inflow conditions. (bottom right) Telescopic sensor towers upstream and downstream of the turbine(s) measure inflow and wake characteristics. Rotating PIV and LF-PIV diagnostics measure local inflow conditions and blade separation. Structural health monitoring diagnostics along with load measurement will operate simultaneously with fluids measurements to provide some of the most detailed data on wind turbine aerodynamics thus far.

III. High Performance Computing (HPC) to Model Coupled Turbine/Atmosphere Interactions and Wake Dynamics

For purposes of improving performance and maximizing lifetimes of wind turbines, it is important to understand the environment to which they are exposed. Certain aspects of their surroundings are represented by high-resolution CFD blade-design codes that resolve the aerodynamic boundary layer of the turbine blade, and others by mesoscale style atmospheric models. However, many of the atmospheric processes affecting wind turbines are not captured by either of these modeling approaches. In order to represent the processes with length scales ranging from blade-chord to wind-farm scales, a new modeling approach, WindBlade has been developed. This new modeling approach is intended to be used to study the interaction between operating turbines and complex flow patterns generated by atmospheric boundary layer processes, local or upstream topography, or even upstream turbines in the context of a wind farm. Implementation of WindBlade in the HPC-based HIGRAD/FIRETEC atmospheric hydrodynamics model has made it possible to explicitly represent the turbulent flow structures over this range of length scales (meters to multiple kilometers) and capture the highly dynamic flows immediately downstream of the spinning turbine blades, with tip speeds in excess of 70 m/s.

With HPC it is possible to approach turbine and turbine wake modeling from a new perspective. Without this level of computational power most models are forced to simplify their representation of the turbine, such as ignoring the transient nature of the spinning blades, ignoring inhomogeneities in the wind field approaching the turbine (i.e. wind shear or turbulence), or deriving an idealized wake function as a function of distance behind the turbine. HPC resources have provided the opportunity to combine a model for a spinning turbine and a highly resolved turbulent wind field with an explicit representation of atmospheric flows with scales ranging over four orders of magnitude. This HPC-based approach is therefore well suited to study the interaction between turbines and the ambient atmosphere, the dynamic loads placed on turbine blades, the development and recovery of turbine wakes, and the interaction between multiple turbines in a wind farm.

D. Turbine/atmosphere interaction

WindBlade uses a combination of Lagrangian and Eulerian techniques to simulate the transport of atmospheric flow features as they approach, interact with, and move downstream of spinning wind turbines. The dynamic two-way interaction between turbine blades and local atmosphere is computed. As kinetic energy is extracted from the winds, the atmospheric flow field responds to forces imparted on it by the turbine. These forces reorient the flow vectors as they pass by the spinning blades and reduce the average speed of the winds behind the turbine. However, these effects are highly transient due to the spinning nature of the blades. In addition to the motions of the spinning blades, the interaction between the turbine and the atmosphere is further complicated in realistic scenarios by the presence of vertical wind shear, directional wind shear, and turbulence at a wide variety of scales. These sorts of features in the atmospheric flow field cause the forces on the turbine to be dynamic and vary widely over the span of the blades. The spatial and temporal variability of the forces imparted by the flow on the blades should be considered in the turbine design process because it certainly affects the wear and tear on turbine components.

Figure 4 illustrates the simulated turbine-induced vorticity behind a rotating turbine. The inflow is a shear layer. In addition to the vorticity induced by the blades, Fig. 4 illustrates the vorticity being shed by the turbine tower, which in turn interacts with the vorticity from the blades.

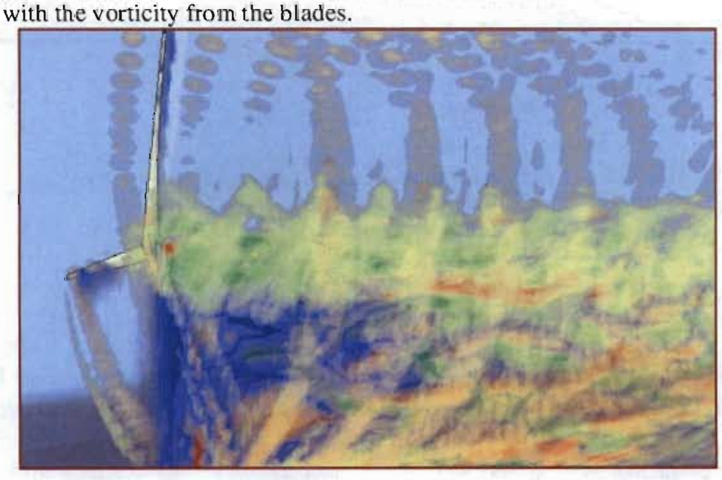

Figure 4: Turbine-induced vorticity in the near vicinity of a spinning turbine

E. Interaction between multiple turbines

Increasing the performance and economic viability of wind farms requires understanding the coupled turbine-atmosphere interactions and resulting turbine-turbine interactions in realistic environments, since this coupling dictates both energy harvest and turbine wear and tear. In a wind farm, ambient atmospheric turbulence interacts with spinning turbines, and the combination produces the mechanism for healing the wind field behind a wind turbine. This combination of ambient and turbine-induced flow patterns determines the environment in which downstream turbines operate. Both the strength of the turbulent structures and their length-scales evolve downstream. It is critical to understand this wake and turbulence evolution behind turbines and how it is influenced by environmental conditions in order to begin to optimize wind farm designs. It is acknowledged that atmospheric turbulence is an important contributor to the performance of wind turbines and wind farms, however until now there have not been sufficient methods to study this interaction. Neither traditional atmospheric models nor turbine-design CFD tools are appropriate for the investigation of the interaction between ambient atmospheric turbulence, turbine-induced turbulence, and turbine performance due to the wide range of critical length scales from blade-chords (meters) to wind farms (tens of kilometers). WindBlade, however, is designed to work across this range of length scales, and thus is being used in a preliminary study of wake dynamics.

WindBlade has been used in an initial study of the integrated impact of blade chord-scale force exchanges between atmosphere and turbines on downstream wakes. Simulations were performed using conditions ranging from idealized laminar winds to empirically-based TurbSim turbulent Low Level Jet (LLJ) conditions. This series of simulations suggest that: i) both ambient and turbine-induced turbulence have significant effects on wake dynamics; ii) the relative impacts of turbine-induced versus ambient turbulence is greater for downstream turbines in a wind farm; and iii) the structure of the wake and turbulent length scales evolve as they are advected downstream of the turbine.

Figure 5 includes an oblique view of the results from a WindBlade simulation. In this simulation, the ambient upstream conditions were derived from the National Renewable Energy Laboratory's (NREL) TurbSim turbulence generator, which creates turbulent winds based on empirical measurements for similar conditions. In this case the wind conditions were similar to those of a LLJ in slightly stable conditions. A passive tracer was emitted from a vertical line spanning each of the rotor discs in order to help visualize the wake structure from these spinning turbines.

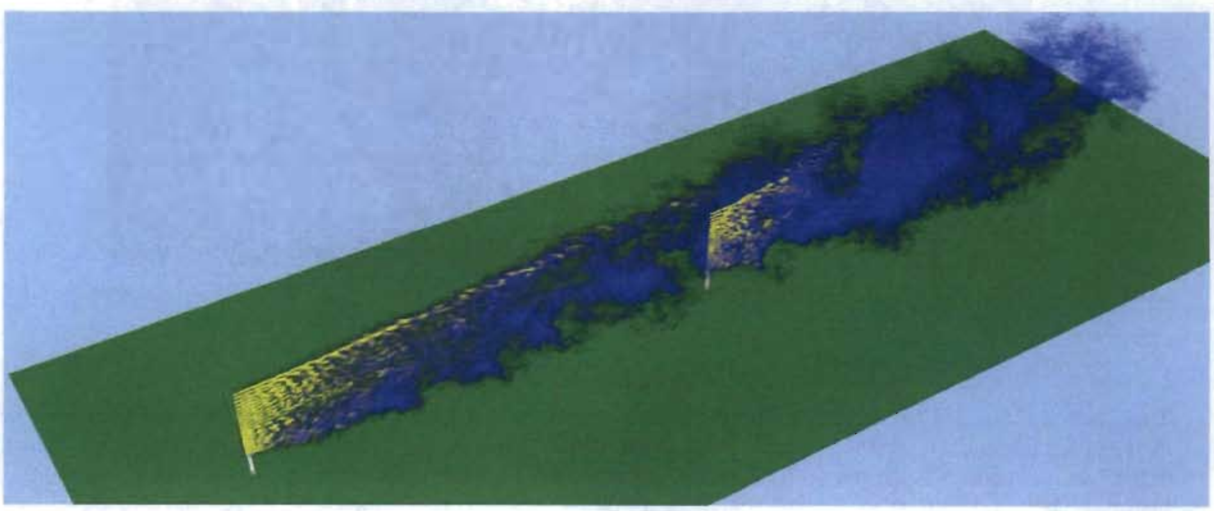

Figure 5: Results from a five-turbine WindBlade simulation. Shading indicates the position of a passive tracer emitted from each of the five turbines for visualization of the wake structure.

F. Complex topography

Wind turbines are being sited in complex topography across the globe for a variety of reasons, including the exposure to concentrated wind resources at strategic sites. The implementation of WindBlade in the atmospheric hydrodynamics model HIGRAD/FIRETEC makes it possible to study the influence of topography and heterogeneous vegetation on the wind fields surrounding turbines. Large upstream and downstream terrain features can have dramatic effects on the amount of energy available to be harvested at a specific location. These effects are frequently studied using a variety of wind resource models similar to meso-scale atmospheric models. In addition to the large-scale impacts of terrain, local terrain features also affect wind profiles, acceleration, mixing, and turbulence in the immediate vicinity of wind turbines. Complex vegetation patterns can also influence the boundary layer and its turbulence.

HIGRAD/FIRETEC, which was originally developed for the purpose of studying wildfire behavior and dispersion in complex settings, provides a validated capability to simulate winds in complex terrain and heterogeneous vegetation. By combining this capability with WindBlade, it is possible to perform high-resolution (~2 m) simulations of winds approaching, interacting with, and passing behind operating wind turbines in complex terrain with heterogeneous vegetation. Preliminary simulations have been performed for multiple turbines in real topographic situations. These simulations have illustrated the dependence of power production on: i) specific turbine positions with respect to the topography; ii) topographic influences on yaw angle and the directional shear of the wind intersecting the turbine; and iii) influences of the topography and vegetation on the structure and extent of the wakes behind the turbines (increased turbulence reduces the extent of the wake regions of the turbines as compared with flat ground.)

Figure 6 illustrates a WindBlade simulation of five hypothetical turbines in complex topography near Las Vegas, NM. In this simulation the vegetation is heterogeneous and based on satellite imagery, but has been omitted from the graphic for clarity sake. An inert tracer has been released from a vertical line near the hub of each turbine to illustrate the wake structure of the turbine.

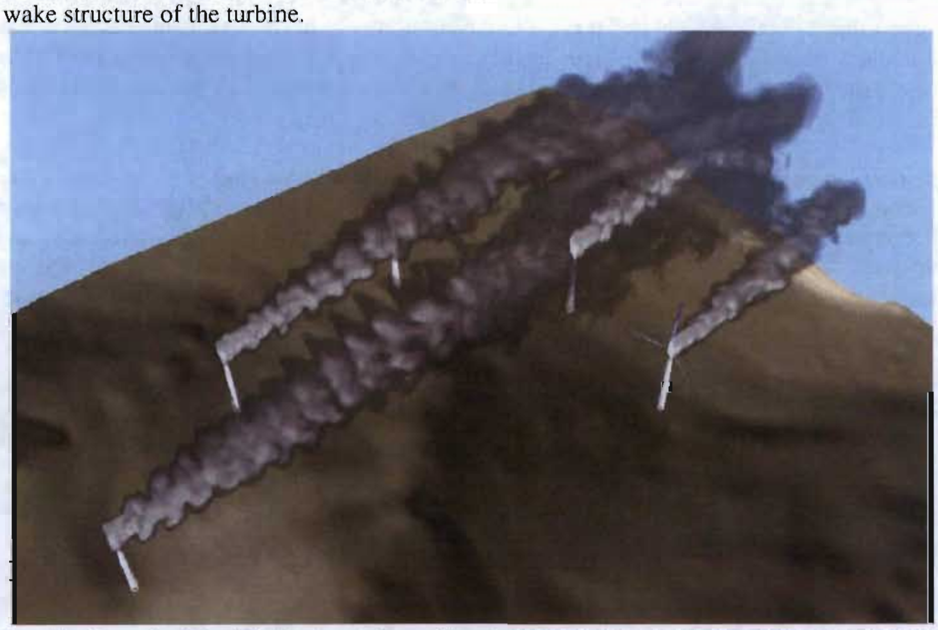

Figure 6. Visualization of a WindBlade simulation of five hypothetical turbines in complex topography near Las Vegas, NM.

IV. Blade Modeling for Aero-Elastic Simulations

This section describes the structural finite element model of a 9 meter CX-100 composite wind turbine blade, developed in support of the Intelligent Wind Turbine (IWT) project at Los Alamos National Laboratory. The CX-100 blade was chosen as the research blade to support the IWT project efforts because of its size, affordability, and history. The CX-100 (Carbon Experimental for a 100 kW turbine) is a 9-meter wind turbine blade developed by Sandia National Laboratories (SNL), and industry partners, in 2002 to investigate the use of carbon in subscale blades. The CX-100 blade has been structurally well-characterized through modal, static, and fatigue testing by SNL and the National Renewable Energy Laboratory (NREL).

The purpose of developing an in-house detailed finite element model of the CX-100 blade is twofold. First, the blade model is intended to function as a workhorse structural model for other aspects of the IWT project. These include the following efforts: blade structural health monitoring; aero-elastically coupled response within the atmospheric hydrodynamics code WindBlade; detailed stress and strain profiles within the blade due to various loadings, with which to develop blade subscale damage, crack propagation, and fatigue models; and application of a formal numerical verification and model validation/uncertainty quantification study.

Second, development of the CX-100 blade was initiated using state-of–the-art engineering simulation tools; specifically, the ANSYS Workbench Environment. The purpose of this was to explore the benefits to blade design and analysis gained by using contemporary simulation and workflow technology tools, but with a well-characterized, well-validated, and well-documented structure such as the CX-100 blade. Existing structural finite element models of the CX-100 blade have previously been developed by Sandia National Laboratory using the conventional ANSYS Classic (recently changed in name to "ANSYS Mechanical APDL", but referred to in this document as Classic) software with a Sandia-developed pre- and post-processing blade design tool known as NuMAD.

G. Structural Dynamics Finite Element Model to Support the IWT Project

The primary purpose of building a detailed and predictive structural finite element model of the CX-100 blade is to support other endeavors within the IWT Project. The completed blade model will support four major ambitions within the IWT project: provide detailed stress and strain locations for sensor placement in support of structural health monitoring of the blade; provide a two-dimensional reduced order, aero-elastic beam element model that can be incorporated into WindBlade - an atmospheric hydrodynamics code that simulates turbine/wind interactions; provide a stress/strain map of the blade with which to develop damage, crack propagation, and fatigue models for subscale structural analyses; and perform a formal model validation/numerical verification effort, and provide data for numerical uncertainty quantification, sensitivity analyses, and resource allocation studies.

H. ANSYS WorkBench, ANSYS DesignModeler, and ANSYS Composite PrepPost

ANSYS is a well-established, well-verified, and commercially available structural finite element analysis software package that has been used widely in industry and academia for 40 years. Over that time it has advanced rapidly to include state-of-the-art physics modeling capabilities that include structural mechanics, fluid dynamics, explicit dynamics, and electromagnetics. Additionally, ANSYS has acquired or developed a number of specific structural mechanics modules to handle rigid body dynamics, composite materials, fatigue, and acoustics analysis. With its version 12.0 release, ANSYS introduced a newly reengineered form of its workflow technology tool called the ANSYS Workbench Platform. Workbench is a framework which hosts a large fraction of ANSYS software products and components in a project schematic diagram. The project geometry, physics simulation tools, boundary conditions, engineering data and solution results are all managed from a single page. Geometry, material properties and model parameters may be reused in other analyses simply by dragging and dropping that information into a new analysis box.

Workbench features include bi-directional, parametric links to all major CAD systems, geometry modeling/repair/simplification using ANSYS DesignModeler, highly-automated meshing, contact detection, and project level parameter variations, to name a few. Parametric variations include CAD geometry dimensions, material properties, boundary conditions, and derived results. The ability to perform parametric variations at a project level page is powerful when considering something as complex as the design and optimization of a wind turbine blade. Changes may be made to geometry, material properties, mesh density, boundary conditions, element types, etc, and the entire suite of physics solutions that have been linked to the blade model is updated automatically to show the changes in the calculated results.

ANSYS DesignModeler, available within the Workbench Platform, is a geometry modeling tool that approaches the sophistication of a high-end CAD package such as SolidWorks or Unigraphics. DesignModeler is a feature-based solid modeler which can be used to create a parametric geometry from scratch or prepare an existing CAD geometry for analysis. Its capabilities uniquely include features and tools specifically intended to prepare a geometry model for analysis. Therefore, if a model has been imported from a CAD system, it can be appropriately de-featured of extraneous geometry not necessary for an analysis, and conversely, features may be added that aid in applying loads and boundary conditions.

Before ANSYS Workbench was available, modeling a wind turbine blade in ANSYS Classic (the conventional ANSYS GUI and solver), would have been time consuming and frustrating. The reasons for this are many. The amount of information needed to define a wind turbine blade in three-dimensions is non-trivial. Complex geometry inputs and subsequent surface descriptions, anisotropic material property definitions, and cloth material layup schedules that vary for different blade regions all combine to make modeling a blade in any detail book-keeping intensive and very time consuming, with little flexibility in the end to modify parameters for optimization studies. Although ANSYS Classic includes composite material definition capability, the interface for describing complex material layups is not user-friendly; the GUI for keeping track of anisotropic material properties, cloth orientation, thicknesses, and stacking orders is so obsolete that creating and maintaining a model as complex as the CX-100 blade requires a significant investment, with little flexibility for making changes.

To address this problem, a software tool called NuMAD (Numerical Manufacturing And Design) was developed by SNL (circa 1998) to simplify the process of creating a three-dimensional finite element model of a wind turbine blade. The design intent of NuMAD was to provide an improved finite element model development environment, enabling users to quickly and easily create three-dimensional models of wind turbine blades, aided by databases of materials, airfoils, and loading conditions, that could be reused with subsequent blade designs. NuMAD is a pre-processor for ANSYS Classic, creating the necessary model information to be used by ANSYS for a particular analysis. There are many features of NuMAD that make blade modeling significantly less cumbersome than trying to model from scratch using ANSYS Mechanical.

In the years since NuMAD was developed, database management, modeling flexibility, workflow technology and GUIs have advanced swiftly. The pre- and post-processing tools available using the ANSYS Workbench Platform are powerful, flexible, and are connected in one project location. For these reasons, we opted to use the ANSYS Workbench Environment for the development of our CX-100 structural finite element model.

I. Modeling of the CX-100 Blade

The point geometry information for the CX-100 9-meter blade was provided by SNL. The geometry definition for the CX-100 blade consists of airfoil profiles at 40 stations along the blade from root to tip. At each station, approximately one hundred points (x and y locations) describe the airfoil shape, consisting of the high pressure and low pressure surfaces of the blade. This information was manipulated using Microsoft Excel to populate a 3 column text file (x, y, z locations) that was read into ANSYS DesignModeler.

Once the blade profiles were read into DesignModeler, the blade was skinned to create the high and low pressure surfaces. Sketches were used to divide the blade into appropriate regions to reflect material build schedules. All geometry content within DesignModeler is parametric, and the entire model updates with any modification to the design. After the blade geometry was complete in DesignModeler, it was moved into Mechanical (within the Workbench Platform) where it was meshed with the appropriate element type.

At this point, ANSYS Composite PrepPost (ACP) was invoked from the Workbench project page. The blade model is opened within ACP to define the material types and layer builds for each region of the blade. In the thickest regions of the blade, the root area, there can be up to 64 layers of individual plies stacked together with different orientations, different thicknesses, and different material properties. The anisotropic material property descriptions, material thicknesses, and fiber orientations were entered into a material data folder in ACP where 'materials', 'fabrics', and 'stack-ups' are stored. 'Elements Sets' with local coordinate systems are used to define which stack-up descriptions are assigned to which regions. The 'Element Sets' are actually inherited from DesignModeler, where they are originally defined as regions. This is important, as a change to a region size or shape in DesignModeler will update all the way to the model in ACP.

At this point, from the Workbench project page, the loads, boundary conditions, and specific analysis options can be applied to the model, and the analysis can be executed. Results may be post-processed in Mechanical or in ACP to see detailed stress and strain results on a layer by layer basis. Figure 7 shows views of the meshed CX-100 blade model, with detailed views of some of the more complicated regions.

J. Status and Future Work

The CX-100 blade model is complete: the geometry and blade modeling is finished to the most accurate level possible using the original blade airfoil coordinate values; region information, material property values, stack-up sequence and orientation have all been defined within the model; static deflection and modal analyses using isotropic material properties have been performed to test mesh continuity and check for overall problems with the model geometry integrity. A formal numerical verification and model validation study of the CX-100 blade model has been initiated.

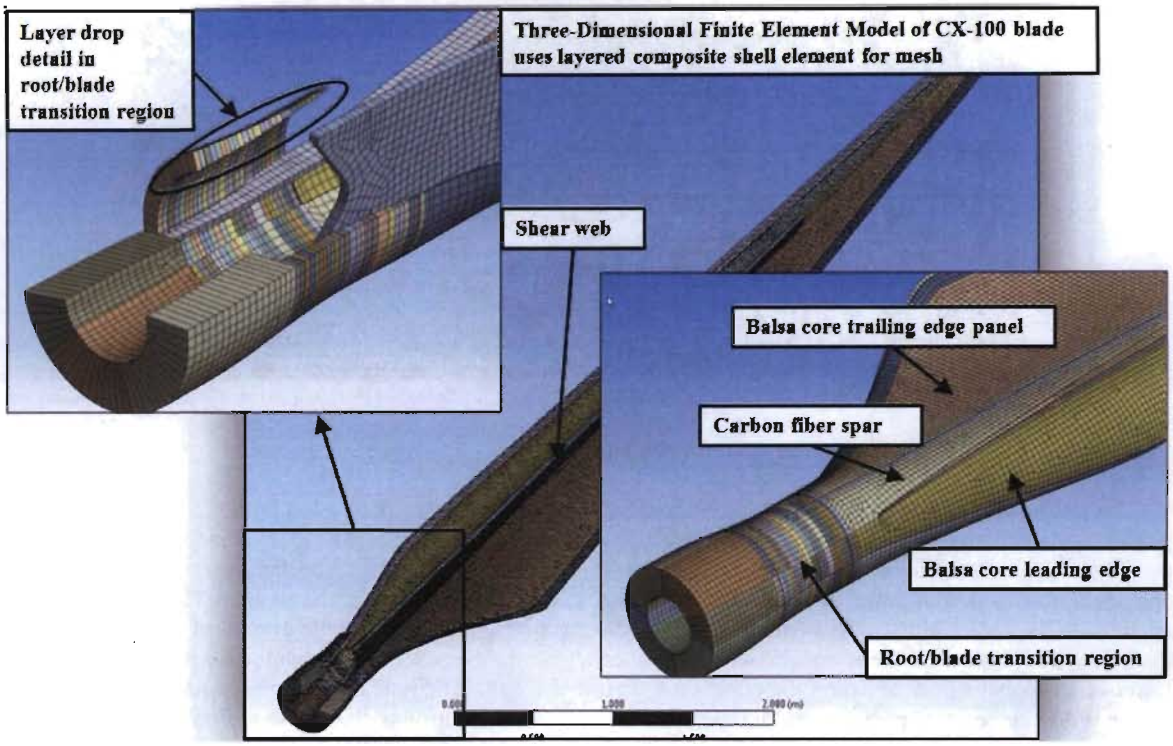

Figure 7. Cross-section views of LANL's Meshed CX-100 Structural Finite Element Model.

V. Multi-Scale Structural Sensing for Health Assessment of a Blade

Monitoring the structural health of wind turbine blades is particularly important as they account for 15-20% of the total turbine cost. In addition, blade damage is one of the most expensive types of damage to repair and can cause serious secondary damage to the wind turbine system due to rotating imbalance created by damage to individual blades. Therefore, the presence of a SHM system incorporated within the design of wind turbines could be used to monitor blade level flaws before they lead system level failures.

The goal of the proposed sensing system is to 1) characterize the dynamic response of the experimental, 9m CX-100 wind blade, 2) develop important design parameters of SHM techniques as they apply to wind turbine blades, and iii) investigate the performance of high-frequency active-sensing SHM techniques, including Lamb wave propagations, frequency response functions, and time series based methods, as a way to monitor the health of a wind turbine blade with piezoelectric sensors. In this study a series of CX-100 blades were dynamically characterized under different boundary conditions, and instrumented with an array of piezoelectric sensors to evaluate several SHM techniques within the laboratory environment. A full-scale fatigue test of a CX-100 wind turbine blade was also performed in collaboration with Sandia National Laboratory (SNL). This examination is a precursor for planned full-scale fatigue testing of the blade and subsequent tests to be performed on an operational CX-100 rotor blade to be flown in the field.

K. Vibration Testing of Turbine Blades

The test structure of a 9-m CX-100 blade is shown in Figure 8. The blade was suspended from metal frames by way of lifting sling support straps at two points. A roving hammer test was used, employing three shear accelerometers (PCB 352C22), two piezoelectric transducers and a modal impact hammer (PCB 086D20). The blade was impacted at several points along the length and chord of the blade in the flap-wise direction. A LDS Dactron data acquisition system was used to collect dynamic data, while MEscope was used for curve-fitting and analysis.

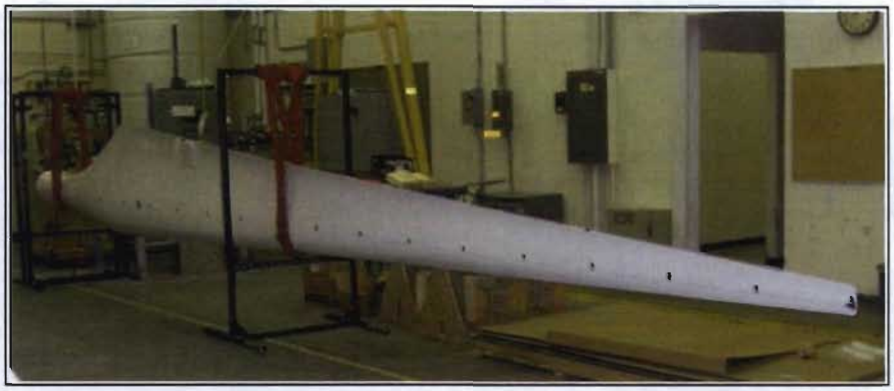

Figure 8: The CX-100 Blade testes under a Free-Free configuration

The testing results are similar to those obtained by in previous studies performed by SNL, and will be used for model validation studies, which is being performed by the authors' research team. The first fundamental modes of the blade were captured using both piezoelectric transducers and traditional accelerometers. The goal of this approach was to demonstrate the multi-scale sensing capabilities of simple piezoelectric transducers. In this application the piezoelectric device can be used to detect the onset and monitor the growth of structural damage in the blade using higher frequency excitations, as will be shown in the next section, while also being used to identify lower-order global modes to assess the effect of structural damage. The fundamental modes measured are shown in Figure 9 As can be seen, piezoelectric transducers are capable of identifying the resonant frequencies of a structure with the same accuracy provided by an accelerometer. This result confirms that, piezoelectric transducers, which have been widely used in SHM, can be efficiently used for monitoring changes in structural dynamics at lower frequency ranges, which allows one can estimate the effect of damage on the system level performance.

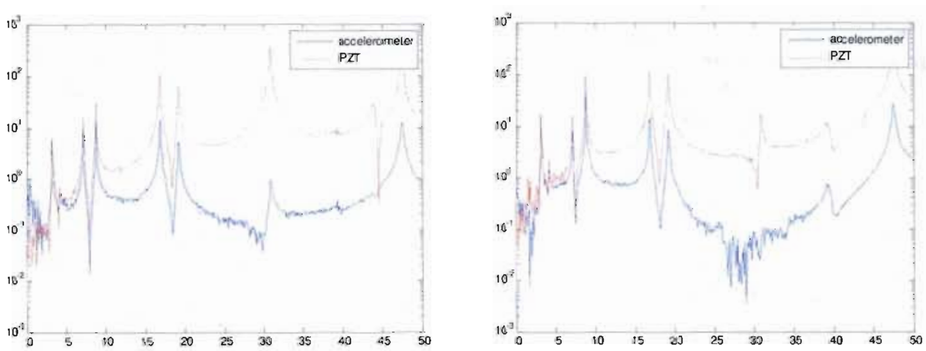

Figure 9: Frequency response functions of the blade up to 50 Hz.

L. SHM using Piezoelectric Active Sensors

The performance of a variety of SHM techniques, based on the use of piezoelectric active-sensors, was investigated to determine the structural integrity of a 9m CX-100 wind turbine blade. Specifically, Lamb wave propagation, impedance based methods, frequency response functions, and a time series based method are utilized to analyze the condition of the wind turbine blade. One of the results using high-frequency response functions are shown in this paper.

The basic concept of high-frequency response functions (FRF) is to use high frequency vibrations to monitor local regions of a structure for changes in the structure's parameters. Damage will alter mass, stiffness, or energy dissipation properties of a system, which, in turn, results in the changes in the high frequency response characteristics of the system[i]. By utilizing piezoelectric active-sensors, FRFs can be measured in the tens to hundreds of kHz ranges, providing a health monitoring technique that is sensitive to small defects within the structure, while not being sensitive to low-frequency operational condition changes of the blade. A specifically designed load frame was used to apply point loads to the test structure, introducing local stiffness changes at various locations, as shown in Figure 10 . The location and intensity of damage was assessed by the response characteristics of each sensor within the piezoelectric sensor array.

Figure 10: Load frame used to apply a point load to the blade

The test was conducted using an excitation frequency bandwidth of 0.5 – 30 kHz on each sensor-actuator combination. The point load (damage 1 illustrated in Figure 11) was applied close to PZT 4, while PZT 1 was used as an actuator. As can be seen in Figure 12, the FRF measured by PZT 2 and PZT 5 were insensitive to the applied stiffness change as they are distant from the damaged area. The influence of damage can be seen for PZT 3 at the frequency range higher than 25 kHz, and as expected, PZT 4 shows the largest changes in response to the local stiffness change.

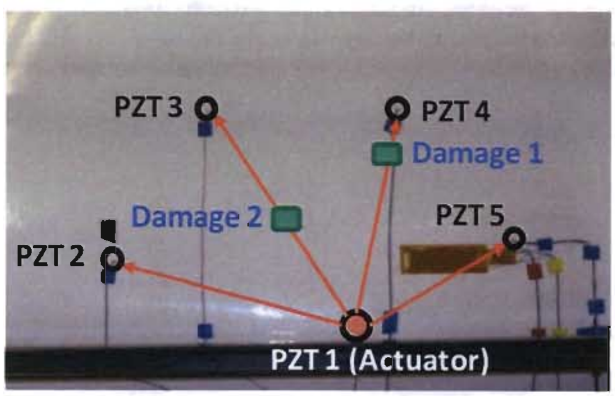

Figure 11: Locations of local stiffness changes

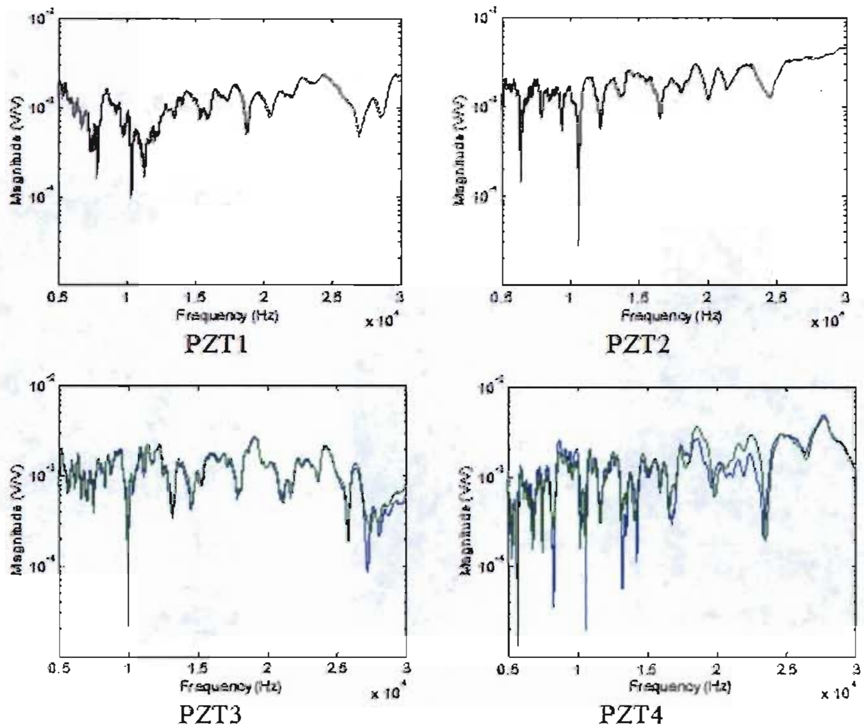

Figure 12: The changes in FRF caused by local stiffness changes

High frequency interrogation techniques were successfully used to detect each of the damage conditions imposed upon the test blade. When coupled with the relatively high damping properties of the host structure, it was possible to locate where damage was imposed by examining the extent to which damage influences the measured response at each transducer location. While the presence of damage can be qualitatively seen in the FRFs shown in Figure 12, a more formal damage index value can be used to quantify system changes before and after damage, as seen in Figure .

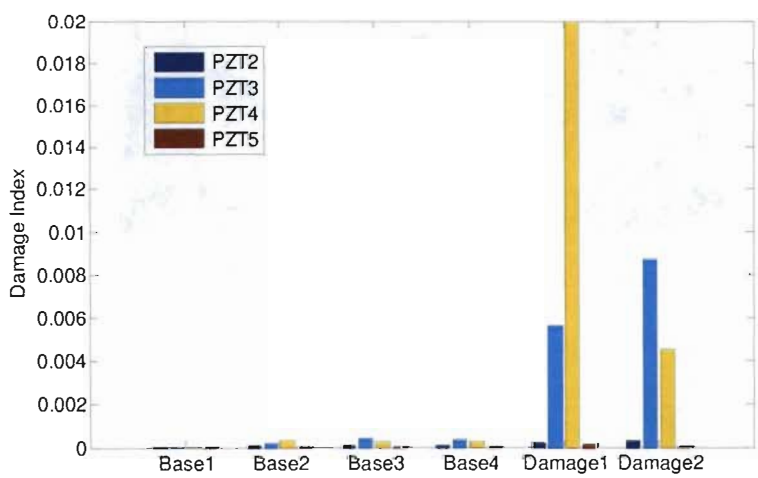

Figure 13: Damage Index using FRFs

It was discovered that the magnitude of the damage index is directly related to the proximity of the propagation path to the damage location and can be utilized to determine the location of the damage with an acceptable degree of accuracy. To summarize, the FRF method is an acceptable structural health monitoring technique for reliably detecting and locating damage in wind turbine blades, and has the potential for limiting the number of sensors required to cover the entire structure. Furthermore, the same sensor can be used to monitor low-frequency response changes, which allows for multi-scale sensing for wind turbine blades.

M. CX-100 Full Scale Fatigue Test

A full-scale fatigue test of a CX-100 wind turbine blade was also performed by SNL at the National Renewable Energy Laboratory (NREL). The LANL instrumentation installed on the SNL 9-meter blade included eleven 1 x 1.5 inch MFC sensors and one 2 x 4 inch MFC actuator. The location of the sensors and the actuator in relation to the blade geometry is also shown in Figure 14. The blade underwent fatigue excitation at 2 Hz for defined intervals, and active-sensing data were collected between sessions while the fatigue excitation source was shut down. These data were collected from the sensing channels at a sampling rate of 60 kHz. Two high-frequency excitation signals were utilized: (1) a 100 to 30,000 Hz chirp signal, and (2) a random excitation signal. For the test, the fatigue damage was visually identified in the root area after 2.3 million cycles.

The collected data were converted to the frequency domain using FFT for the start of the fatigue cycling and at each cessation thereafter. Baseline FRF data was collected for the blade in the pristine condition, and was used to evaluate the system response from data collected at each subsequent test interval. Correlation coefficients between the baseline and new datasets were used as a feature to track the progression of structural change over the course of the fatigue test. The values of the correlation coefficients calculated at periodic intervals throughout the course of the test are shown in Figure 15 for MFC transducers 2-4. Note from Figure 14, that channel 4 was mounted at 2 meters, near the root of the blade, and that channel 3 was mounted at 3 meters, where the aerodynamic portion of the blade begins. Channel 2 is located close to the actuator. Based on the significant increase in the damage index value, it is apparent that the structural change is stronger at the root, which is also a high strain region of the blade. It should also be noted that the damage index values shows a large increase after 1.5 million cycles. It is speculated that the fatigue damage would have been initiated much earlier than when visually identified. Channel 3 shows the relatively large changes as the blade approaches 2 million cycles. Channel 2 did not show any noticeable changes, as the fatigue damage is distant from this sensor location, confirming the damage localization capability of piezoelectric active-sensing.

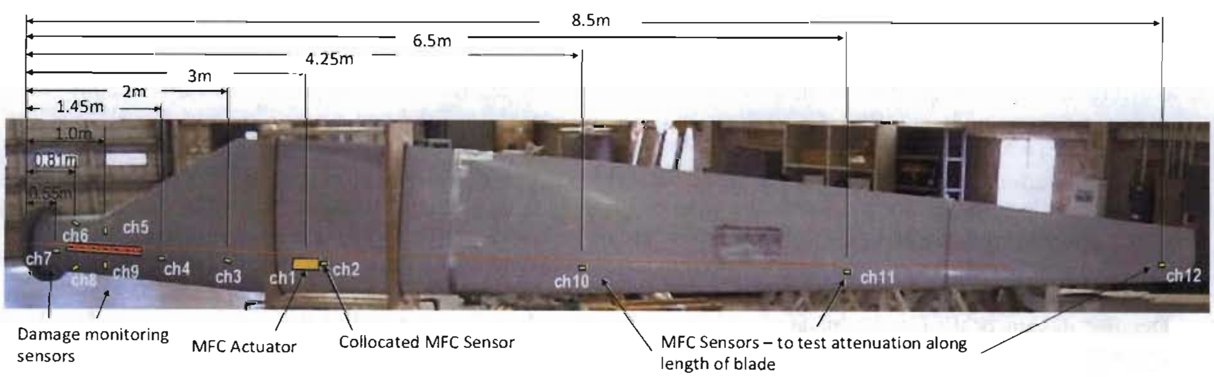

Figure 14: Overview of the fatigue test setup (courtesy of Sandia National Laboratory) A single MFC actuator is used to excite the blade, and 11 MFC sensors are used to measure the signal

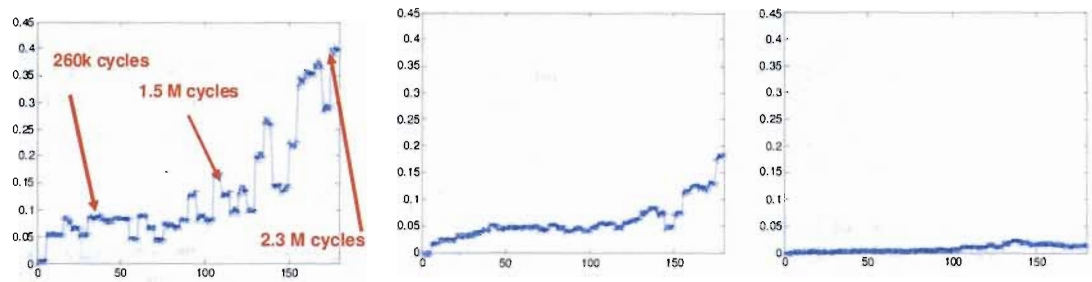

Figure 15: Correlation coefficient changes during the fatigue test channel 4 (left), channel 3 (middle), and channel 2 (right). Each value represents the result of one test.

VI. Summary

Los Alamos National Laboratory's Intelligent Wind Turbine project has made substantial progress in the last 1.5 years in applying diagnostics and simulation tools originally developed for mission-related applications to the problem of wind turbine reliability. A new LANL wind turbine field station is under construction (expected completion July, 2011), and will be used for generating state-of-the-art aerodynamic and structural data for the validation of numerical simulations. The facility will also provide a unique opportunity to study turbine-turbine interactions at a level of detail that has not been achieved previously. Substantial progress has been achieved in the areas of aerodynamic measurement and diagnostics, aero-elastic supercomputer simulations of wind farms in complex terrains, modeling of the CX100 blade (in collaboration with Sandia), and structural health monitoring.

Large Field of View Particle-Image Velocimetry (LF-PIV) diagnostics capable of very large fields of view (4.3m x 1.0m) have been demonstrated in gas flows. These represent one of the largest PIV fields of view achieved thus far and promise to provide high fidelity mean and turbulence measurements around wind turbines. Accuracy tests on a laboratory scale apparatus showed that LF-PIV is capable of better than 2% accuracy on flows with moderate accelerations (~100g), placing LF-PIV as a prime candidate for studying blade tip vortices and near field inflow and wake structures.

A novel Rotating-PIV diagnostic has also been developed to measure dynamical stall and separation around wind turbine blades. This diagnostic is capable of measuring blade boundary layer and separated flows over all phases of blade rotation. Uniquely, these diagnostics also provide a non-intrusive method for local inflow measurement under conditions of turbulence and gust. The LF-PIV and R-PIV diagnostics along with standard three-axis sonic anemometers will be used at the LANL field station to provide detailed aerodynamics and structural data on turbine-turbine interactions with unprecedented accuracy under full wake and partial wake immersions.

A new modeling and simulation framework, WindBlade, capable of resolving scales ranging from blade scales (2m) to planetary boundary layer scales (several Kms) has been developed at LANL. Simulations performed on LANL's high-performance supercomputing platforms show that the scalable code is capable of resolving blade load fluctuations under turbulent inflow conditions in compex topographies. Many components of this framework have been extensively evaluated at LANL under various previous programs. Thus, in comparison to newly developed codes, this code has been validated and verified under complex scenarios offering high confidence in its results. Currently, efforts are underway to integrate and test WindBlade on turbines with aero-elastic blades.

Detailed models of the CX100 blade have been developed at LANL incorporating the multi-layer manufacturing process of the composite blade. This model is intended to function as a workhorse structural model for our aero-elastic simulation framework, for blade structural health modeling, blade subscale damage modeling, crack propagation and uncertainty quantification. In particular, it is important to note that this design was accomplished using a commercially available code to enable a wide use of this model.

Three different structural health monitoring diagnostic techniques have been developed and tested on blades (Lamb wave propagation, frequency response functions and a time-series predictive model). They have each yielded sufficient damage detection capability. Tests on a 9-m blade under fatigue testing at the NREL facility has shown that our inexpensive active sensing nodes are capable of detecting and tracking fatigue induced crack growth in blades.

In the next phase of the project, these diagnostic and simulation developments will be tied in together to provide a unified framework for understanding turbine-turbine interactions and wind turbine reliability under complex inflow conditions.

Acknowledgment

The support of Department of Energy's Energy Efficiency and Renewable Energy office through Grant# EB2501030 (PI: B. J. Balakumar) and LANL's Laboratory Directed Research and Development Office through Grant# 20100040DR (PI: C. Ammerman) are gratefully acknowledged. The enjoyable collaborations with our colleagues from Sandia National Laboratories, Albuquerque is gratefully acknowledged.

REFERENCES

---

[1] "20% Wind Energy by 2030", DoE Report GO-102008-2567 (2008).

[2] Walford, "Wind Turbine Reliability: Understanding and Minimizing Wind Turbine O&M Costs", Sandia National Laboratories Report, SAND2006-1100 (2006).

[3] Hill et al., "Wind Turbine Reliability: A Database and Analysis Approach," SAND2008-0983 (2008).

[4] Poulos G., Personal correspondence, Senior Meteorologist, Clipper Windpower Development, Inc.

[5] Angelou et al., "Doppler Lidar Mounted on a Wind Turbine Nacelle – UPWIND deliverable D 6.7.1", Riso-Report-1757 (2010).

[6] Manwell et al., "Wind Energy Explained: Theory, Design and Application", 2nd Edition, John-Wiley & Sons (2009).

[7] "Summary of IEA RD&D Wind – 51st Topical Expert Meeting", (2007).

[8] Kelley et al., "Comparing Pulsed Doppler LIDAR with SODAR and Direct Measurements for Wind Assessment," National Renewable Energy Laboratory Report NREL/CP-500-41792 (2007).

[9] Antoniou et al., "Offshore Wind Profile Measurements from Remote Sensing Instruments," in EWEC 2006, Athens, Greece (2006).

[10] Courtney et al., "Testing and Comparison of Lidars for Profile and Turbulence Measurements in Wind Energy," IOP Conference Series: Earth and Environmental Science **1** (2008).

[11] Fischer et al., "Pitot Tube Designed for High Frequency Inflow Measurements on MW Wind Turbine Blades", EWEC, France (2009).

[12] Kit et al., "In Situ Calibration of Hot-Film Probes Using a Collocated Sonic Anemometer: Implementation of a Neural Network", J. Atmospheric and Oceanic Technology **27** (2010).

[13] Adrian R. J., Westerweel J., Particle Image Velocimetry, Cambridge University Press (2011).

[14] Vermeer et al., "Wind Turbine Wake Aerodynamics", Prog. Aerospace Sciences **39** (2003).

[15] Adrian R.J. (Arizona State University), Yamauchi G. (NASA Ames), Personal Communication.

[16] Hecht E., "Optics", Addison-Wesley (2002).

[17] Pol S., Balakumar B.J., "Large Field of View Particle-Image Velocimetry (LF-PIV): Design and Performance", in review AIAA-ASM (2012)

[18] Park, G., Rutherford, C.A., Wait, J.R., Nadler, B.R., Farrar, C.R.,"The Use of High Frequency Response Functions for Composite Plate Monitoring with Ultrasonic Validation," AIAA Journal, 43, 2431-2437(2005).